International Journal of Pharmacy and Biological Sciences-IJPBS™ (2019) 9 (1): 1125-1137
Online ISSN: 2230-7605, Print ISSN: 2321-3272
Research Article | Biological Sciences | Open Access | MCI Approved
UGC Approved Journal

In Silico Antimicrobial Activity of Bioactive Compounds from Roots of *Pisonia Grandis* R. Br

Murugesan Rajeswari[1*], Natchimuthu Santhi[1] and Shubashini K Sripathi[2]

[1]Assistant Professor, Department of Biochemistry, Biotechnology and Bioinformatics Avinashilingam Institute for Home Science and Higher Education for Women, Coimbatore – 641043.

[2] Professor, Department of Chemistry, Avinashilingam Institute for Home Science and Higher Education for Women, Coimbatore – 641043.

Received: 10 Oct 2018 / Accepted: 10 Nov 2018 / Published online: 1 Jan 2019
Corresponding Author Email: rajeswari.murugesan81@gmail.com

Abstract

Aim: *Pisonia grandis* R.Br (Nyctaginaceae) widely distributed throughout India and reported to have anti-microbial, anti-inflammatory, anti-diabetic, diuretic, analgesic and wound healing properties. The focus of the study is to evaluate the antimicrobial activity of the compounds reported in roots of *Pisonia grandis.* **Methods:** Glide (Schrödinger Software suite) was used to perform molecular docking studies to assess the antimicrobial activity of the compounds present in the roots of *Pisonia grandis*. **Results:** The compounds reported in roots of *Pisonia grandis* namely β-sitosterol, leptumerol , quercetin, 3-Hydroxy-5,7,2' trimethoxy-6,8-dimethylflavone, 3,5,2'-trihydroxy-7,3'-dimethoxy-6,8-dimethylflavone, 5,7,2'-trihydroxy-3'-methoxy-6,8-dimethylflavone, 7,2'-dihydroxy-5,6-dimethoxy-8-methyl isoflavone, 6,2'-dihydroxy-5,7-dimethoxy-8- methyl isoflavone, 6,8 dimethylsogenistein, 5,7,2'-trihydroxy-6-methoxy-8-methyl isoflavone, IrilinA and 5,7,2'-trihydroxy-6,8-dimethylflavanone were found to have good docking score and binding energy with antimicrobial targets namely dihydrofolate reductase, dihydropteroate synthase, topoisomerase, isoleucyl tRNA synthetase, D-alanine-D-alanine ligase, enoyl-acyl carrier protein reductase and chorismate synthase. **Conclusion:** The bioactive compounds from *Pisonia grandis* were found to have good binding interaction with antimicrobial target proteins. The present docking study validates the results of Suthhivaiyakit *et al*., who stated that the free phenolic group at C-2` position is essential for antibacterial activity.

Keywords
*A*ntibacterial, Docking, Glide, *Pisonia*, Prime-MMGBSA.

*****

INTRODUCTION

Tribal extensively use the various parts of the *Pisonia grandis* R.Br in the preparation of different folk medicines. The plant has numerous bioactive compounds such as pinitol, allantoin, β sitosterol, α-spinasterol, β sitosterol glucoside, octacosanol, dulcitol and quercetin and they are reported to have antidysenteric, antidiabetic, anti-inflammatory, analgesic, antifungal and antidiabetic properties [1, 2].

The presence of structural information of target proteins and ligands enhances the success rate of drug discovery process. Early drug discovery phase includes structure-based drug design to increase the success rate in drug lead identification. Advances in target identification increased the development of target-based drug discovery method [3]. Based on the targets, antibiotics are classified as inhibitors of cell wall synthesis, protein synthesis, nucleic acid synthesis, and metabolites. The drugs developed against single protein target were failed due to drug resistance because an even single missense mutation in protein target will alter the binding efficacy of drugs. Therefore, the multi-target hypothesis has raised considerable importance with the development of new potential compounds. Owing to this advantage in the treatment of complex diseases linked to drug resistance issues. In this present study, from the root of *Pisonia grandis* were analyzed for their antibacterial activity in multiple protein targets.

MATERIALS AND METHODS

The antibacterial activity of the flavonoids from *Pisonia grandis* are checked by doing molecular docking studies using Glide (Schrödinger Software suite 2015). A pre-requisite of obtaining the highest quality docking result is to use protein and ligand structures prepared using protein preparation wizard and LigPrep (Schrödinger Software suite 2015).

Target proteins

Table 1 shows the selected target proteins for the present study. The 3D structure of the target proteins was downloaded from the PDB database (http://www.rcsb.org/). The missing hydrogen atoms and incorrect bond order assignment were done correctly using the tools Protein Preparation Wizard of Maestro and Prime of Schrödinger Software suite.

Table 1: List of antimicrobial target proteins

Target Protein	Organism	PDB	Reference
Dihydrofolate reductase	*Staphylococcus aureus*	4XE6	Not published
Dihydropteroate synthase	*Streptococcus pneumonia*	2VEG	[4]
Topoisomerase	*Staphylococcus aureus*	3TTZ	[5].
Isoleucyl tRNA synthetase	*Thermus thermophiles*	1JZQ	[6].
D-alanine-D-alanine ligase	*Thermus thermophiles*	2ZDQ	Not published
Enoyl-acyl carrier protein reductase	*Mycobacterium tuberculosis*	3FNE	[7].
Chorismate Synthase	*Streptococcus pneumonia*	1QXO	[8].

Ligands

The compounds used for the present study were β-sitosterol (C1), leptumerol (C2), quercetin (C3), 3-Hydroxy-5,7,2' trimethoxy-6,8-dimethylflavone (C4), 3,5,2'-trihydroxy-7,3'-dimethoxy-6,8-dimethylflavone (C5), 5,7,2'-trihydroxy-3'-methoxy-6,8-dimethylflavone (C6), 7,2'-dihydroxy-5,6-dimethoxy-8-methyl isoflavone (C7), 6,2'-dihydroxy-5,7-dimethoxy-8- methyl isoflavone (C8), 6,8 dimethylsogenistein (C9), 5,7,2'-trihydroxy-6-methoxy-8-methyl isoflavone (C10), IrilinA (C11) and 5,7,2'-trihydroxy-6,8-dimethylflavanone (C12) and are shown in Fig.1. The 3D structure of flavonoids reported from Pisonia grandis [9] was built using Build Panel of Maestro. The ligand structures were prepared using LigPrep (Schrödinger Software suite) to produce single, low energy confirmation with correct chirality.

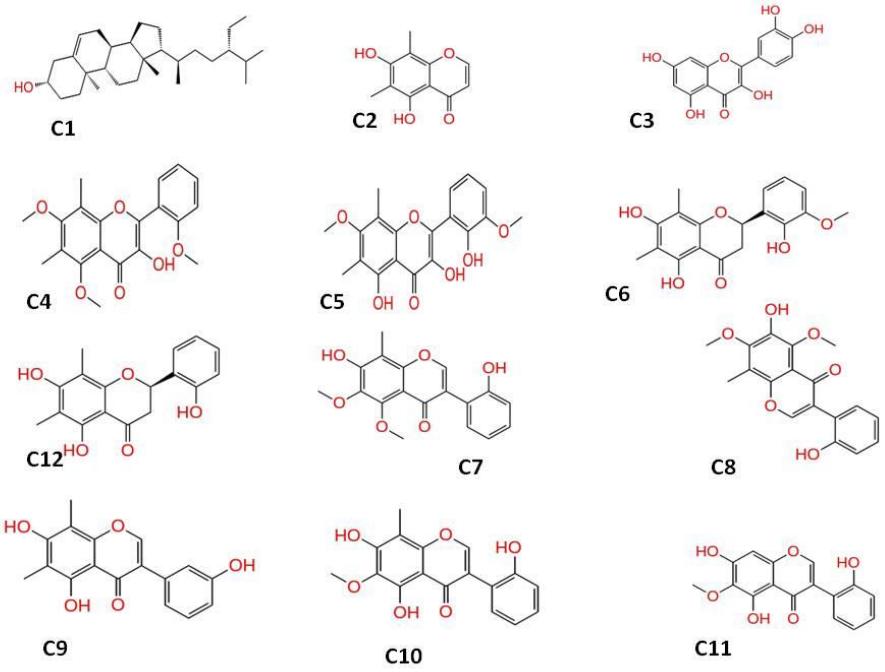

Fig. 1: Structure of selected compounds from *Pisonia grandis*

Receptor grid generation

The exclusion of the ligand from the receptor region of the target protein by defining the receptor grid using the Receptor Grid Generation panel of the tool Glide. This will enable various ligand poses to bind within a predicted active site during docking. The grid was generated keeping the default parameters of van der Waals scaling factor of 1.0 and partial charge cutoff value of 0.25 subjected to OPLS 2001 force field. A cubic box with the dimension of 14Aº x 14Aº x 14Aº centered on the centroid of the active site residue was generated.

Docking

The Standard Precision (SP) mode of Glide was used for docking the ligands with target proteins. The binding site of the target protein was defined with receptor grids. Atom in the target protein and ligands with a fixed partial charge of ≤0.25 and scaling factor of 1.0 has been applied to the concept of *Van der Waals* radii. During the initial phase of the docking calculation, the maximum poses generated from the variables were fixed to 10000, and the best variable which set some poses per ligand that enters the minimization was 10. At the end of the docking process, one pose per ligand was set. Using Glide Score function, the best-docked structures were selected. The E-model score, which is also considered, and it is the combination of G-score, *van der Waals*, coulombic interaction and the strain energy of the ligand.

Pose rescoring using Prime MM-GBSA (Molecular Mechanism Generalized Born Surface Area)

The prime MM-GBSA was applied to calculate ligand binding energies and ligand strain energies for the ligand and the receptor to scoring function values to improve docking accuracy. The molecular docking combined with MM-GBSA, not only predict to binding- free energy of the compounds but also provided novel strategy for lead optimization. MM-GBSA is a method that combines OPLSA molecular mechanics energies (EMM), and SGB solvation model for polar solvation (GSGB), and a non-polar solvation term (GNP) composed of the non-polar solvent accessible surface area and *van der Waals* interactions. Here, the Glide pose viewer file of the best conformation chosen was given as the source in Prime MM-GBSA simulation. The total free energy of binding:

$$\Delta G_{bind} = G_{-complex} - (G_{-protein} + G_{ligand}), \text{ where } G = EMM + GSGB + GNP$$

RESULTS AND DISCUSSION

Validation of the docking studies

Many methods are available for validating the docking programs, and scoring functions [10] [11]. One of the commonly used methods is redocking of the native ligand into the receptor site of the complex structure. The orientation predicted to be the most favourable for the known ligand can be compared to the actual crystallographically determined orientation by calculating the root mean square deviation (RMSD) between the location of the ligands in the predicted and crystallographically determined binding mode. If the docking programme positions the ligand in the same manner in the receptor as in the crystal structure, a low RMSD value will be obtained and vice versa. Typically, the RMSD value of 2 Å is accepted as a good pose [12].

Superposition panel of the Maestro (Schrodinger software suite) was used to calculate the root-mean-square deviation (RMSD) between native structure and the predicted conformation.

The RMSD value for all the docked target proteins with co-crystallised ligand was not more than 2.0 Å except dihydrofolate reductase indicates that the ligand is placed in the correct orientation by the docking program (Table 2).

Table 2: Validation of docking program

Target Protein	Class	PDB ID	Co-crystallized ligand	RMSD Å	Glide Score
D-alanine-D-alanine ligase	A	2ZDQ	ATP (natural substrate)	1.68	-11.19
Isoleucyl tRNA synthetase	B	1JZQ	ILA (inhibitor)	0.69	-8.10
Topoisomerase	C	3TTZ	O7N (drug)	1.64	-7.55
Dihydrofolate reductase	D	4XE6	06U (inhibitor)	2.16	-6.22
Dihydropteroate synthase	D	2VEG	PMM (drug)	0.81	-8.09
Enoyl-acyl carrier protein reductase	E	3FNE	8PC (inhibitor)	0.45	-7.51
Chorismate Synthase	F	1QXO	EPS (natural substrate)	1.21	-10.37

Note: A - Inhibitors of cell wall synthesis; B-Inhibitors of protein synthesis; C-Inhibitors of nucleic acid synthesis; D-Antimetabolites; E-Inhibitors of Fatty acid synthesis; F-Inhibitor of aromatic amino acid synthesis

Binding of selected ligands into the active pocket of antimicrobial targets

Enoyl-acyl carrier protein reductase

Bacterial fatty acid biosynthesis differs from the mammalian counterpart and is the energy-intensive process that is essential for the formation of the bacterial membrane. Enoyl-acyl carrier protein reductase (ENR) catalyzes the reduction of trans-2-enoyl ACP to Acyl-ACP in the final process of the elongation cycle of fatty acid synthesis. This step is the rate controlling step in fatty acid elongation providing a solid rationale for targeting the enzyme as an antimalarial and antibacterial target [13]. There are three types of inhibitors for ENR: bi-substrate inhibitors (Isoniazid), inhibitors binding to NAD(P)-ENR complex (Triclosan) and NAD(P)H-ENR complex (AFN-122, CG400462) [14]. The crystal structure of ENR (PDB ID: 3FNE) used as the target has coordinates of the 1.98 resolution structure include NAD^+/8PC inhibitor complex. Nicola *et al.* stated that inhibitors for ENR interact with NAD^+ in the active pocket of the enzyme [15]. Therefore, this cofactor was retained in the active site during docking. The ENR of *Mycobacterium tuberculosis* consists of homo tetramer containing four active sites. The bioactive compounds from *P. grandis* root are targeted to Triclosan analogue bound to pocket underneath fatty acyl substrate binding site which is predominantly lined by hydrophobic groups from the side chains of Tyr158, Phe149, Met199, Trp222, Leu218, Met155, Met161, Gly192, and Pro193.

Table 3 depicts the Gide Score, E-model, H-bond interaction and Prime MM-GBSA binding energy of selected compounds with ENR. From the Fig. 2a, it is evident that all the compounds bind to the same active pocket as the native ligand (8PC). However, the C8 (blue) has the same orientation as 8PC (purple) and having good docking score of -7.2 with pi-pi interaction. Except for C8, all other compounds are oriented towards concerning dichloro phenoxy ring of 8PC. C1 (β-sitosterol) does not have any interactions with ENR because of its hydrophobic active site. All the C- methylated isoflavones (C7, C8, C9, C10 and C11) were found to have the docking score between -6.0 and -7.2 and forms H-bond with Ala198 except C7 and C8. The C-methylated flavonones (C4, C5, C6 and C12) expressed docking score between -5.6 to -6.0 and form H-Bond with either Gln100 and Gly96 except for C4.

Table 3: Molecular docking results for selected bioactive principles from the roots of *P. grandis* with Enoyl-acyl carrier protein reductase

Ligand		Glide Score	Glide Emodel	H bond		Pi-Pi interaction	ΔG_{bind} (Kcal/mol)
				BB	SC		
β-sitosterol	C1	-	-	-	-	-	-
Leptumerol	C2	-5.2	-35.8	-	-	-	-23.4
Quercetin	C3	-6.1	-51.8	Met98	-	-	-44.9
C-methyl flavone	C4	-6.0	-46.5	-	-	-	-10.9
	C5	-5.9	-48..5	Gln100	-	-	-44.0
	C6	-5.6	-47.9	Gln100	-	-	-44.1
	C12	-5.7	-39.9	Gly96		Phe149	-38.8
C-methyl isoflavone	C7	-6.0	-46.21	-	-	-	-30.5
	C8	-7.2	-37.3	-	-	Phe149	-26.8
	C9	-6.4	-49.3	Ala198	-	-	-41.7
	C10	-6.6	-49.3	Ala198	-	-	-40.3
	C11	-6.9	-54.6	Gly96, Ala198	-	-	-33.2

BB: H-Bond with a backbone of proteins
SC: H-bonds with a side chain of amino acids

Chorismate Synthase

In bacteria, fungi, plants and apicomplexan parasites, chorismate, the final product of the shikimate pathway is the branch point in the biosynthesis of the folic acid, vitamin K, ubiquinone and aromatic amino acid that are essential for that organisms. The absence of the shikimate pathway in human makes it an attractive target for the development of new antimicrobial agents. Chorismate synthase (CHS) catalyzes the conversion of 5-enoyl pyruvyl shikimate-3-phosphate (EPSP) to chorismate in the presence of cofactor reduced FAD [16]. The EPSP binding site of CHS is the hydrophilic and extremely basic environment with six arginine and two histidine residues. The basic and polar residues of the substrate binding site of CHS are Ser9, His10, Arg45, Arg48, His110, Ser132, Ala133, Arg134, and Arg337. The flavonoids were docked into the substrate (EPSP) binding site of enzyme chorismate synthase from *Streptococcus pneumonia* (1QXO). All the compounds bind to the active pocket of CHS in the same orientation as EPSP (Figure 2b). Table 4 depicts the Glide Score, E-model, H-bond interaction and prime MMGBSA binding energy of selected compounds with CHS. The compound C3 is having lowest docking score of - 6.2.

The compound C3 is having five hydroxyl groups and forms the hydrogen bond with basic amino acids (Arg39, Arg107, and Arg337) and pi-pi interaction with Arg45. The C-methylated isoflavones (C7, C8, C9, C10 and C11) were found to have lower docking score (-5.0 to -5.6) compared to the C-methylated flavones (-4.1 to -4.9) except C12 which gave a score of -5.2. Among the C-methylated isoflavones, the docking score decreased as the number of methoxy substituent increased, C9 (-5.6) does not have methoxyl group whereas C7 (-5.2) and C8 (-5.0) are dimethoxy isoflavones. The β-sitosterol forms H-bond with Ala133 and Arg45, and leptumerol (C2) does not show any H-bond interaction. All the flavones and isoflavones form the Hydrogen bond with either one of three arginine residues namely Arg337, Arg107 and Arg48.

Table 4: Molecular docking results for selected bioactive principles from the roots of *P. grandis* with Chorismate Synthase

Ligand		Glide Score	Glide Emodel	H bond		Pi-Pi Interaction	ΔG_{bind} (Kcal/mol)
				BB	SC		
β-sitosterol	C1	-4.2	-38.4	Ala133	Arg45	-	-
Leptumerol	C2	-4.8	-37.9	-	-	-	-
Quercetin	C3	-6.2	-61.3	Arg337	Arg107* Arg39*	Arg45	-35.1
C-methyl flavone	C4	-4.6	-46.7		Arg48, Asp339	-	-44.3
	C5	-4.9	-48.9		His10, Arg48	-	-46.3

	C6	-4.1	-45.8	Asp339	-	-	-32.3
	C12	-5.2	-54.2	Arg337	Arg107	Arg45	-
C-methyl isoflavone	C7	-5.2	-49.7	Arg337	H_2O		-35.2
	C8	-5.0	-48.3		Hip10, Arg48, H_2O	-	-
	C9	-5.6	-50.1	Arg337	H_2O		-33.4
	C10	-5.3	-50.1		Lys83, Asp80, His10, Arg48, H2O	-	-32.6
	C11	-5.4	-48.9		Lys83, Asp80, His10, Arg48, H2O	-	-35.6

BB: H-Bond with the backbone of proteins
SC: H-bonds with a side chain of aminoacids
***- denotes two H-bond with the same amino acid**

Isoleucine tRNA synthetase (IleRS)

The Aminoacyl tRNA synthetase played an essential role in the biosynthesis of protein and made as a promising antimicrobial target. Mupirocin [17] and Benzoxaboroles [18] are a class of aminoacyl tRNA synthetase inhibitors successfully developed in recent times. Mupirocin binds to the natural substrate binding site of IleRS, and it mimics the aminoacyl-AMP (aa-AMP) intermediate. In general, an aa-AMP analogue potently inhibits the corresponding aminoacyl tRNA synthetases, and it lacks specificity. However, analogues of mupirocin failed in clinical trials due to poor absorption and lack of specificity, and therefore restricted to topical use [19]. In the present study selected active principles from *P. grandis* root are docked into the aa-AMP analogue N-[isoleucinyl]-N'-[adenosyl]-diaminosufone binding site of IleRS from *Thermus thermophilus* PDB ID: (IJZQ). The residues present in the binding site of aa-AMP analogues are Gly45, Pro46, His54, Gly56, His57, Gln59, Asp85, Glu550, Gly551, Glu553, Gln554, Trp558, His558, Gly582, Lys583 and Ile584.

The GlideScore, E-model, H-bond interaction and prime MM-GBSA binding energy of selected compounds with IleRS is depicted in Table 5. The quercetin (C3) was found to have lowest docking score of -7.3 compared to C-methylated flavonone and isoflavone which may be due to the hydrophobicity of active pocket of isoleucyl tRNA synthetase (Figure 2c). It is also noted that all the flavones and isoflavones form Hydrogen bond with Glu550.

Table 5: Molecular docking results for the selected bioactive principles from the roots of *P. grandis* with Isoleucine tRNA synthetase

Ligand		Glide Score	Glide Emodel	H bond		Pi-Pi	ΔG_{bind} (Kcal/mol)
				BB	SC		
β-sitosterol	C1	-4.2	-40.8	Leu52	-	-	-12.6
Leptumerol	C2	-5.9	-44.8	-	Asp85, His57	-	-19.1
Quercetin	C3	-7.3	-73.0	-	Asp85, Glu553, Glu550, His581	-	-34.1
C-methyl flavone	C4	-5.7	-41.4	Gly551	Gln554, Glu550	His57, His54	-31.8
	C5	-5.4	-49.7	-	His54, Thr48, Asp85, Glu550	Trp518	-29.6
	C6	-5.8	-49.0	Gly45 Thr48	Asp85,Thr48	His57	-31.5
	C7	5.9	-54.5		Glu550, Asp85	His57	-36.8
C-methyl is flavone	C12	-5.3	-57.6	-	Asp85, Gln554, Glu550	Trp518	-28.6
	C8	-5.8	-45.4	Thr48	His57, Glu550	-	-42.5

Ligand		Glide Score	Glide Emodel	H bond		Pi-Pi	ΔG_{bind} (Kcal/mol)
				BB	SC		
	C9	-5.8	-56.9	-	Thr48, -Glu550	-	-36.2
	C10	-5.1	-43.4	-	Thr48, Glu550	-	-31.2
	C11	-5.2	-56.1	-	Thr48,Glu550		-29.5

BB: H-Bond with a backbone of proteins
SC: H-bonds with a side chain of aminoacids
***- denotes two H-bond with the same amino acid**

D-alanine-D-alanine ligase

D-alanyl-D-alanine is a key component of the bacterial cell polysaccharide peptidoglycan, and it maintains cell wall stability by cross-linking the peptidoglycan chains. D-alanine-D-alanine ligase (DDL) with the help of ATP hydrolysis synthesized the dipeptide D-alanine-D-alanine [20]. The ATP is bound to the free enzyme followed by the binding of D-Ala_1 and phosphorylation of the amino acid carboxylate resulting in the generation of acyl phosphate intermediate. The acyl phosphate intermediate is attacked by D-ala_2 to yield dipeptide D-alanyl-D-alanine [21]. D-cycloserine (D-4-amino-3-isooxazolidone) is a structurally analogue to D-alanine inhibited biosynthesis of dipeptide D-alanyl D-alanine and was developed as DDL inhibitor [22]. There are different categories of the inhibitors for DDL that have been described: Analogs of D-alanine, analogues of product (dipeptide), transition state analogues, ATP competitive inhibitor and inhibitor discovered by *in silico* screening or modelling [23, 24]. In the present study, *P. grandis* active principles were docked into the ATP binding site of DDL from *Thermus thermophilus*. The ATP binding site of the DDL consist of polar amino acids namely Glu13, Phe151, Lys153, Gly 158, Ser 159, Ser160, Ile163, Glu189, Lys190, Ala191, Leu192, Glu197, Tyr218, Phe222, Tyr223, Lys228, Tyr229, Arg268, Glu270, Phe272, Asn281, Glu282, Asn284 and Gly289.

Table 6 portrays the GlideScore, E-model, H-bond interaction and prime MM-GBSA binding energy of the selected compounds with DDL. All the compounds were found to have good docking score ranging from -8.5 to -6.0. The compounds C2, C10, and C11 showed lowest docking score of -8.2, -8.5 and -8.4 respectively. All the C-methylated isoflavone compounds were found to have a docking score of -8.5 to -7.7 except C8 which gave a score of -6.3. The presence of methoxy group in the fifth position of flavonoid ring may hinder the interaction of C8 with the ATP binding site of DDL (Fig. 2d).

Table 6: Molecular docking results for the selected bioactive principles from the roots of *P. grandis* with D-alanine-D-alanine ligase

Ligand		Glide Score	Glide Emodel	H bond		Pi-Pi interaction	ΔG_{bind} (Kcal/mol)
				BB	SC		
β-sitosterol	C1	-6.0	-39.9		Glu282	-	9.91
leptumerol	C2	-8.2	-54.3	Leu192*	Glu189, Lys153	Phe5	-45.9
quercetin	C3	-7.2	-74.5	-	Glu282, Lys153, Asp270	Lys228(Pi cation), Phe272, Phe151	-52.4
C-methyl flavone	C4	-7.0	-57.5	Tyr223	-	Lys228(Pi cation) Phe 151	-52.7
	C5	-6.8	-52.8	Tyr223	Ser160	Phe151	-62.4
	C6	-6.9	-59.2	Tyr223	Glu197	Phe151	-36.4
	C7	-7.0	-61.5	Tyr223, Leu192	Glu197	Phe151, Lys228 (pi cation)	-57.7
C-methyl isoflavone	C12	-7.3	-54.9	Tyr223, Leu192	Glu197	Phe151	-23.9
	C8	-6.3	-58.8		Glu282, Asn284,	Lys228(Pi cation)	-36.3

				Glu197	Phe 151	
C9	-7.7	-65.3	Tyr223	Glu197, Glu282	Phe 151	-46.3
C10	-8.5	-71.2	Tyr223	Glu197, Glu282, Lys116	Phe 151	-45.7
C11	-8.4	-88.4	Tyr223,	Lys116, Glu282, Glu197	Phe 151	-46.3

BB: H-Bond with a backbone of proteins
SC: H-bonds with a side chain of aminoacids
***- denotes two H-bond with the same amino acid**

Folate synthesis pathway

Tetrahydrofolate (THF) produced by the folate biosynthetic pathway has a key role in one-carbon transfer reactions in the biosynthesis of biomolecules, such as nucleotides and amino acids. The enzymes, which play a major role in the synthesis of THF, are dihydropteroate synthase (DHPS), dihydrofolate synthase (DHFS) and dihydrofolate reductase (DHFR). DHPS catalyzes the condensation of *p*-aminobenzoic acid (pABA) to dihydropterin pyrophosphate to form pteroic acid, and DHFS catalyzes the addition of glutamate to pteroic acid to form dihydrofolate (DHF). DHFR catalyzes the reduction of DHF to form tetrahydrofolate (THF). The absence of the folate synthesis pathway in higher organisms makes it a particularly attractive target for antibacterial drug design [25].

Dihydropteroate Synthase

The sulfonamide class of antibacterial drugs was the first class of synthetic antibacterial agents to be used successfully clinically since the 1930's, and it targets the enzyme dihydropteroate synthase (DHPS). The DHPS is absent in Human, which is an advantage from a drug design point of view. Sulfonamides function as a competitive inhibitor for DHPS substrate pABA which prevents bacterial growth and cell division [26]. However, significant resistance has been developed over the years to these drugs, due to the resistance mutation in pABA binding pocket. The presence of the heterocyclic ring in sulfa drugs leads to the position of these compounds outside the DHPS substrate envelope. Therefore, the mutations at Phe33 and pro69 can impede the binding of the drug to DHPS substrate site [27].

In this study, bioactive compounds from the root of *P. grandis* were docked into the pterin binding pocket of DHPS from *Streptococcus pneumonia* (2VEG) complex with pterin-6-YL-methyl-monophosphate (PMM). DHPS possesses a classic ($\beta\alpha$) TIM barrel structure consisting of 13 helices and nine strands. The cavity of DHPS is lined by nonpolar residues namely Ile15, Asn-17, Asp91, Asn110, Ile112, Met135, Asp211, Phe216, phe231, Lys237, Arg282, and His284. Table 7 depicts the Glide Score, E-model, H-bond interaction and prime MMGBSA binding energy of the selected compounds with DHPS.

The Fig. 2e shows that all the compounds were found to dock with the same site as of PMM (purple colour) except C1 which is a steroid and has a different orientation (red colour) and a hydrogen bond with Arg236. All the flavonoids had a hydrogen bond interaction with either one of the amino acid namelyArg282, Asn110, Phe206, Asp201, Glu55, Asn17, Asp91 and Leu237. In addition to hydrogen bonds the flavonoids C2, C3, C6, C8, C9, C10 and C11 exhibited pi-pi interaction with Arg282 and Phe206. Among the is flavones, C8 was found to have lowest docking score of -5.5.

Table 7: Molecular docking results for the selected bioactive principles from the roots of *P. grandis* with Dihydropteroate Synthase

Ligand		Glide Score	Glide Emodel	H bond		Pi-Pi interaction	ΔG_{bind} (Kcal/mol)
				BB	SC		
β-sitosterol	C1	-4.1	-36.3	-	Arg236	-	-40.9
Leptumerol	C2	-4.9	-30.6	-	Lys237*, Ash91	Arg282,	-21.9
Qquercetin	C3	-5.1	-53.9	-	Arg282*, Asn110, Phe206,	Arg282, Phe206	-43.2

					Asp201, Glu55		
C-methyl flavone	C4	-4.6	-46.4	-	Arg282, Asn17	-	-33.81
	C5	-4.6	-49.9	-	Arg282*, Asn17	-	-35.6
	C6	-4.8	-45.9	Gly205	Lys237,	Arg282, Phe206	-41.6
	C12	-4.5	-40.9	Gly205, Arg236	Lys237	Arg282, Phe206	-32.5
C-methyl isoflavone	C7	-5.4	-48.9	-	Arg282* Asn17		-36.3
	C8	-5.5	-48.9	-	Lys237*, Ash91	Arg282, Phe206	-39.6
	C9	-4.8	-42.4	-	Arg282*, Asn17	Arg282(Pi cation)	-28.4
	C10	-5.2	-45.6	-	Arg282*, Asn17	Arg282(Pi cation)	-31.6
	C11	-5.2	-50.4	-	Asn110*, Asn17, Arg282, Asp201	Arg282, Phe206	-41.3

BB: H-Bond with a backbone of proteins
SC: H-bonds with a side chain of amino acids
***- denotes two H-bond with the same amino acid**

Dihydrofolate reductase

Dihydrofolate reductase (DHFR), a key enzyme of the folate pathway which reduces 5,6-DHF to 5,6,7,8-THF using NADPH as a cofactor. The Human DHFR sequence is 30% similar to *E. coli* DHFR thereby providing as an attractive antimicrobial target. Inhibitors of DHFR are successful agents for the treatment of various infectious diseases as well as for cancer (Methotrexate-MTX) [28]. DHFR inhibitor such as trimethoprim, brodimoprim, tetroxoprim and iclaprim are in clinical use. These compounds compete with the pteridine moiety of DHF for binding to the enzyme [29]. Structural studies showed that DHFR is a monomeric molecule and has two subdomains, the adenosine-binding subdomain, and the loop subdomain. The adenosine-binding subdomain binds the adenosine moiety of NADPH. The active site is present between the two subdomains where folate and NADPH bind [30].

The molecular docking study was carried out with DHFR enzyme complexed with NADPH and 6-ethyl-5-[(3R)-3-[3-methoxy-5-(pyridin-4-YL) phenyl] BUT-1-YN-1-YL] pyrimidine-2,4-diamine (06U) from *Staphylococcus aureus (4XE6).* The DHFR from *S. aureus* consists of 5 helices and 13 strands. The flavonoids from *P. grandis* were docked into the DHF binding site, and the active pocket is lined with polar and non-polar amino acids namely Leu5, Val6, Ala7, Arg12, Gln19, Leu20, Asp27, Leu28, Val 31, Thr46, Ser49, Ile50, Leu 54, Phe92, Thr111, and Tyr126. Table 8 depicts Glide Score, E-model, H-bond interaction and prime MMGBSA binding energy of selected compounds with DHFR. The binding pocket of all selected ligands with DHFR is shown in Fig. 2f.

Table 8: Molecular docking parameters of selected bioactive principles from the roots of *P. grandis* with Dihydrofolate reductase

Ligand		Glide Score	Glide Emodel	H bond		ΔG_{bind} (Kcal/mol)
				BB	SC	
β-sitosterol	C1	-5.9	-29.2	-	-	-39.2
leptumerol	C2	-6.2	-43.2	-	Asp27	-38.4
quercetin	C3	-6.6	-55.6	Phe92	Asp27	-39.1
C-methyl flavone	C4	-6.4	-52.3	-	-	-52.6
	C5	-6.1	-56.7	-	Phe92, Ser49	-47.8

	C6	-7.1	-56.5	Ser49	Asp27	-42.8
	C12	-8.5	-57.4	Phe92	Ser49	-
C-methyl isoflavone	C7	-7.8	-64.70	-	-	-
	C8	-7.5	-61.9	-	Phe92	-57.1
	C9	-8.3	-64.1	Ser49 Asp27	-	-56.1
	C10	-7.8	-62.3	Phe92, Ser49	-	-57.1
	C11	-7.3	-33.1	Phe92	Ser49	-

BB: H-Bond with a backbone of proteins
SC: H-bonds with a side chain of amino acids

All the flavonoids were found to have good docking score of -8.5 to -6.1 except steroid (C1) with a docking score of -5.9. The C9 and C12 showed lowest docking score of -8.3 and -8.5 respectively. In comparison to other flavones and isoflavones, C9 and C12 do not possess methoxy substituent which may contribute to better interaction and lowest docking score. The flavones and isoflavones possessing free 2'OH show good docking score compared to C4 (-6.4) and C5 (-6.1) which lacks 2'OH. 2'OH of C4 is methylated whereas, in the case of C5, 2'OH may form intra molecular hydrogen bonding with 3' methoxy group.

DNA gyrase (GyrB)

DNA gyrase is an essential enzyme for bacteria and inhibition results in the disruption of DNA synthesis and cell death. DNA gyrase (Topoisomerase II) is a heterotetramer of two subunits (GyrA and GyrB) and introduces negative supercoils in DNA ahead of the replication fork, thereby relieving torsional strain during replication. GyrB subunits correspond to ParC and ParE in Topoisomerase IV which separates linked catenanes of two DNA molecules during replication.

Type II topoisomerase has emerged as an antibacterial target. The quinolone class of antibacterial drugs acts on the DNA gyrase and topoisomerase IV. Quinolones stabilize gyrase-DNA cleavage complex by binding to an interface between DNA, GyrA and GyrB and thereby inhibiting enzyme-mediated ligation of cleaved DNA [31]. Aminocoumarins inhibit gyrase by competing with ATP, thereby blocking the ATPase activity of the GyrB subunit [32]. However, increasing prevalence of resistant bacterial strain against quinolones and poor pharmacokinetics of coumarin drugs, urge the development of new inhibitors against DNA gyrase.

In the present study molecular docking of active principles from *P. grandis* was carried out in the ATP binding pocket of the GyrB subunit of DNA gyrase. The GyrB from *Staphylococcus aureus* (3TTZ) complexed with pyrrolamide an ATP competitive inhibitor was download from the PDB website. The active site residue of GyB complexed with pyrrolamide inhibitor are Asn44, Ser45, Glu58, Glu81, Arg84, Gly85, Ile86, Pro87, and Arg144. The secondary structural composition of GyrB of *Staphylococcus aureus* is 34% helices and 28% beta sheets. The Glide Score, E-model, H-bond interaction and prime MMGBSA binding energy of selected compounds with GyrB is depicted in table 9. The binding pocket of all selected ligands with GyrB is shown in Fig. 2g.

The C3, C5 and C6 were found to have the lowest docking score of -7.8, -7.6 and -7.5 respectively. The C-methylated flavones were found to possess good interaction with GyrB subunit compared to C-methylated isoflavones which showed docking score of -6.7 to -6.2. The possible reason may be due to the steric hindrance caused by isoflavonoid ring in ATP binding site of GyrB. Among the C-methylated flavones, C4 provided dock score of only-6.5 which may be due to the absence of hydrogen bond formation with the protein.

Table 9: Molecular docking parameters of selected bioactive principles from roots of *P. grandis* with DNA gyrase

Ligand		Glide Score	Glide Emodel	H bond		ΔG_{bind} (Kcal/mol)
				BB	SC	
β-sitosterol	C1	-6.1	-	-	Asp57	106
leptumerol	C2	-6.4	-56.2	Asn54	-	22.4
quercetin	C3	-7.8	-81.8	Gly85	Asn54, Asp81	-1.64

C-methyl flavone	C4	-6.5	-66.5	-	-	18.1
	C5	-7.6	-80.5	-	Asp81	-24.21
	C6	-7.5	-70.2	-	Asn54	39.1
	C12	-6.8	-66.02	-	Asp81	1.8
C-methyl isoflavone	C7	-6.5	-67.8	-	Asp81	10.9
	C8	-6.5	-69.2	-	Asp81	9.3
	C9	-6.7	-64.7	-	Asp81	2.6
	C10	-6.2	-64.0	-	-	41.7
	C11	-6.4	-65.7	-	Asp81	7.01

BB: H-Bond with a backbone of proteins
SC: H-bonds with a side chain of amino acids

Table 10: Comparison of Glide Score of bioactive principles from the roots of *P. grandis* with selected antimicrobial protein targets

Ligand	Glide Score						
	ENR	CHS	IleRS	DDL	DHPS	DHFR	GyrB
C1	-	-4.2	-4.2	-6.0	-4.1	-5.9	-6.1
C2	-5.2	-4.8	-5.9	-8.2	-4.9	-6.2	-6.4
C3	-6.1	-6.2	-7.3	-7.2	-5.1	-6.6	-7.8
C4	-6.0	-4.6	-5.7	-7.0	-4.6	-6.4	-6.5
C5	-5.9	-4.9	-5.4	-6.8	-4.6	-6.1	-7.6
C6	-5.6	-5.2	-5.8	-6.9	-4.8	-7.1	-7.5
C12	-5.7	-4.1	5.9	-7.0	-4.5	-7.6	-6.8
C7	-6.0	-5.2	-5.3	-7.3	-5.4	-7.8	-6.5
C8	-7.2	-5.0	-5.8	-6.3	-5.5	-7.5	-6.5
C9	-6.4	-5.6	-5.8	-7.7	-4.8	-8.3	-6.7
C10	-6.6	-5.3	-5.1	-8.5	-5.2	-7.8	-6.2
C11	-6.9	-5.4	-5.2	-8.4	-5.2	-7.3	-6.4

CONCLUSION

The bioactive compounds of *P. grandis* roots were found to have better binding interaction with antimicrobial protein target lined with polar amino acid (dihydrofolate reductase, D-alanine-D-alanine ligase and topoisomerase) compared to the active site having hydrophobic side chain (Enoyl-acyl carrier protein reductase, dihydropteroate synthase and isoleucyl t-RNA synthetase). The flavanol quercetin was found to have good docking score with all the selected protein targets ranging from -7.3 to 5.1 however, it has poor cell permeability. The lipophilic methylated flavones and isoflavones have good interaction with selected antibacterial protein targets; methylation doesn't reduce the antimicrobial activity. It can also be observed that flavones and isoflavones having 2'OH and lacking 3'OMe group namely C7 to C12 have shown better interaction with selected protein compared to C4 to C6 except in case of topoisomerase. The present molecular docking study validates the results of Suthhivaiyakit *et al.* stated that the free phenolic group at C-2' position is essential for antibacterial activity [9].

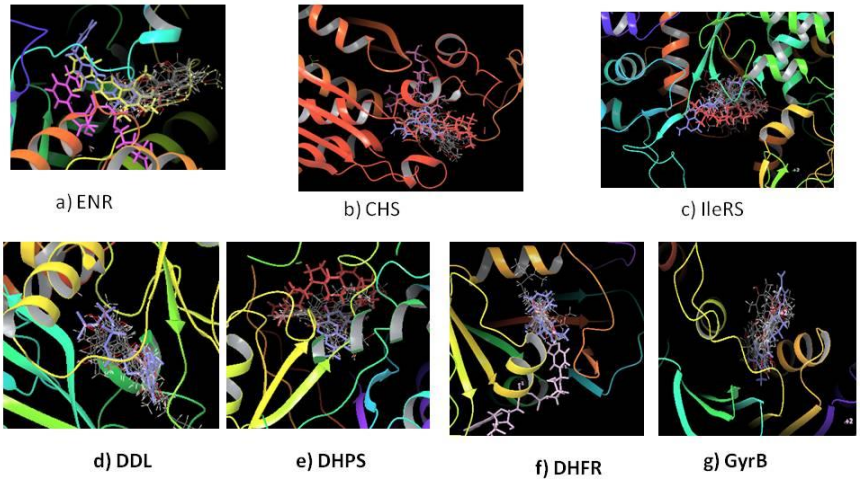

The cocrystallized ligand of protein targets – purple color; β-sitosterol – red color; Cofactors – magenta color

Figure 2: Binding of selected ligands to the active pocket of the antimicrobial targets. a) Enoyl-acyl carrier protein reductase (ENR) b) Chorismate Synthase (CJS) c) Isoleucine tRNA synthetase (IleRS) d) D-alanine-D-alanine ligase (DDL) e) Dihydropteroate Synthase (DHPS) f) Dihydrofolate reductase (DHFR) g) DNA gyrase(GyrB).

REFERENCES:

1. Sripathi SK, Gopal P and Lalitha P. Allantoin from the leaves of *Pisonia grandis*, RBr. Int. J. Pharm. Life Sci 2011a; l (2):815–817.
2. Sripathi SK, Poongothai G and Lalitha P. Antidiabetic agent: Pinitol from the leaves of *Pisonia grandis* RBr. J. Nat. Remedies 2011b; 11:39–43.
3. Lionata E, Spyrou G, Vassilatis DK and Cournia Z. Structure-based virtual screening for drug discovery: Principles, applications and recent advances 2014; 14(16):1923-38.
4. Levy C, Minnis D and Derrick JP. Dihydropteroate synthase from *Streptococcus pneumoniae*: structure, ligand recognition and mechanism of sulfonamide resistance. Biochem J. 2008; 412(2):379-88.
5. Sherer BA, Hull K, Green O, Basarab G, Hauck S, Hill P, et al. Pyrrolamide DNA gyrase inhibitors: optimization of antibacterial activity and efficacy, Bioorg Med Chem Lett. 2011; 21(24):7416-20.
6. Nakama T, Nureki O and Yokoyama S. Structural basis for the recognition of isoleucyl-adenylate and an antibiotic, mupirocin, by isoleucyl-tRNA synthetase. J Biol Chem, 2011; 276(50):47387-93.
7. Freundlich JS, Wang F, Vilcheze C, Gulten G, Langley R, Schiehser et al. Triclosan derivatives: towards potent inhibitors of drug-sensitive and drug-resistant *Mycobacterium tuberculosis*, Chem Med Chem. 2009; 4(2): 241-8.
8. Maclean J and Ali S. The structure of chorismate synthase reveals a novel flavin binding site fundamental to a unique chemical reaction, Structure 2003; 11(12): 1499-511.
9. Sutthivaiyakit S, Seeka C, Wetprasit N and Suthhivaiyakit P. C-methylated flavonoids from *Pisonia grandis* roots. Phytochemistry Letters 2013; 6:407-11.
10. Cole JC, Murray CW, Nissink JW, Taylor RD and Taylor R. Comparing protein-ligand docking programs is difficult. Proteins. 2005; 60:325–332.
11. Jain AN. Bias, reporting, and sharing: computational evaluations of docking methods. J. Comput. Aided Mol. Des. 2008; 22:201–212.
12. Kramer B, Metz G, Rarey M and Lengauer T. Ligand docking and screening with FLEXX. Medicinal Chemistry Research 1999; 9(7):463-478.
13. Morde VA, Shaikh MS, Pissurlenkar RRS and Coutinho EC. Molecular modelling studies, synthesis and biological evaluation of *Plasmodium falciparum* enoyl-acyl carrier protein reductase (pfENR) inhibitors, Mol Divers 2009;13:501-17.
14. Yao J and Rock CO. Resistance mechanism and the future of bacterial enoyl-acyl carrier protein reductase (FabI) antibiotics. Cold Spring Harb Perspect Med 2016; 6(3): a027045.
15. Nicola G, Smith CA, Lucumi E, Kuo MR, Karagyozov L, Fidock DA, Sacchettini JC and Abagyan R. Discovery of novel inhibitors targeting enoyl-acyl carrier protein reductase in Plasmodium falciparum by structure-based virtual screening Biochem Biophys Res Commun 2007; 6(3):686-91.
16. Dias MV, Ely F, Palma MS, de Azevedo WF Jr, Basso LA and Santos DS. Chorismate synthase: an attractive target for drug development against orphan diseases. Curr Drug Targets 2007; 8(3): 437-44.
17. Chain EB and Mellows G. Pseudomonic Acid. Part 1. The structure of Pseudomonic acid A, a novel antibiotic produced by *Pseudomonas fluorescens.* J. Chem. Soc. Perkin 1 1977; 1(3):294–309.
18. Baker SJ, Zhang YK, Akama T, Lau A, Zhou H, Hernandez V, Mao W. Alley, M.R, Sanders V and

Plattner JJ. Discovery of a new boron-containing antifungal agent, 5-fluoro-1,3-dihydro-1-hydroxy-2,1-benzoxaborole (AN2690), for the potential treatment of onychomycosis. J. Med. Chem 2006; 49:4447–50.

19. Hu QH, Liu RJ, Fang ZP, Zhang J, Ding YY, Tan M, Wang M, Pan W, Zhou HC and Wang ED. Discovery of a potent, benzoxaborole based anti-pneumococcal agent targeting leucyl-tRNA synthetase. Scientific Reports 2013; 3:2475.
20. Huynh KH, Hong M, Lee C, Tran HT, Lee SH, Ahn YJ, Cha SS and Kang LW. The crystal structure of the-alanine-D-alanine ligase from *Acinetobacter baumannii* suggests a flexible conformational change in the central domain before nucleotide binding. J. Microbiol 2015; 53(11):776-82.
21. Healy VL, Mullins LS, Li X, Hall SE, Raushel FM and Walsh CT. d-Ala-d-X ligases: evaluation of d-alanyl phosphate intermediate by MIX, PIX and rapid quench studies. Chem Biol 2000; **7**:505–514.
22. Neuhaus FC and Lynch JL. The enzymatic synthesis of D-alanyl-D-alanine. III. On the inhibition ofD-alanyl-D-alaninesynthetase by the antibiotic D-cycloserine. Biochemistry 1964; 3(4):471–480.
23. Skedelj V, Arsovska E, Tomasic T, Kroflic A, Hodnik V, Hrast M *et al*. 6-Arylpyrido[2,3-d] pyrimidines as novel ATP-competitive inhibitors of bacterial D-alanine: D-alanine ligase. PLoS One 2012; 7(8): e39922.
24. Tytgat I, Colacino E, Tulkens PM, Poupaert JH and Vost MP. DD-ligases as a potential target for antibiotics: Past, Present and Future. Curr. Med. Chem. 2009; 16:2566–80.
25. Capasso C and Supuran CT. Sulfa and trimethoprim-like drugs – antimetabolites acting as carbonic anhydrase, dihydropteroate synthase and dihydrofolate reductase inhibitors. J. Enzyme Inhib Med. Chem 2014; 29(3):379–387.
26. Hevener KE, Yun MK, Qi J, Kerr ID, Babaoglu K and Hurdle JG. Structural Studies of Pterin-Based Inhibitors of Dihydropteroate Synthase. Journal of Medicinal Chemistry 2010; 53(1):166–77.
27. Yun MK, Wu Y and Li Z. Catalysis and sulfa drug resistance in dihydropteroate synthase. Science 2012; 335:1110–14.
28. Desai NC, Trivedi AR and Khedkar VM. Preparation, biological evaluation and molecular docking study of imidazolyl dihydropyrimidines as potential *Mycobacterium tuberculosis* dihydrofolate reductase inhibitors, Bioorg Med Chem Lett 2016; 26(16): 4030-5.
29. Hawser S, Lociuro S and Islam K. Dihydrofolate reductase inhibitors as antibacterial agents. Biochem. Pharmacol 2006; 71:941–8.
30. Kovalevskaya NV, Smurnyy YD and Polshakov VI. Solution structure of human dihydrofolate reductase in its complex with trimethoprim and NADPH. J Biomol NMR 2005; 33:69–72
31. Ketron AC, Aldred KJ, Lindsey H and Osheroff N. Gyrase and Topoisomerase IV as targets for antibacterial drugs, Living Reference Work Entry. Molecular Life Sciences 2014; 1-5.
32. Maxwell A and Lawson DM. The ATP -binding site of type II topoisomerases as a target for antibacterial drugs. Curr Top Med Chem 2003; 3:283-303.